RICE UNIVERSITY

An Extended Cavity Diode Laser in Red Wavelengths

Wenmiao “Wendy” Liu

Advisor: Dr. Thomas C. Killian

2013/4/1

Contents

1. Introduction

In this project, we fabricate and characterize a 689nm External Cavity Diode Laser. This laser allowed stable, single-mode operations, and was to be used for Doppler cooling on the $^3P_1 \rightarrow {}^1S_0$ line of strontium, which can serve as part of a cooling and trapping system to generate dense, ultracold samples.

1.1 Laser Cooling

Our lab cools and traps Strontium atoms to acquire ultra-cold (a few mK), dense atomic samples. The key in this process is to decelerate the atomic beam by laser cooling. This is usually accomplished by directing a near resonant laser beam toward the atomic beam [4]. According to Doppler's effect, the atoms will absorb laser photons which are somewhat red-shifted from the atomic resonance frequency. The atoms absorb these photons and are therefore slowed down by the head-on collisions with the photons. The absorbed photons are then spontaneously emitted to random directions, so the emissions, overall, not change the atomic velocity. After many of such absorption-emission processes, the atoms will experience a net momentum change toward the direction of laser propagation. On average, this momentum change can be described as a damping force that the photons exert on the atom sample:

$$F = \hbar k \frac{\Gamma}{2} \frac{I/I_0}{1 + I/I_0 + \left[\frac{2(\delta - \mathbf{k}\cdot\mathbf{v})}{\Gamma}\right]^2}$$

In this equation, F is the average damping force the atoms exerperience of the laser. $\Gamma = \tau^{-1}$ is the decay rate of the atom population in the excited state, the inverse of natural lifetime. I/I_0 is the normalized intensity of the laser. $\delta = w_{laser} - w_{beam}$ is the shift of laser frequency from the natural resonant frequency of the atom. $\mathbf{k} = 2\pi/\lambda$ is the wave vector of the photon. v is the velocity with which the atom recoils after absorbing or emitting a photon.

As seen from the equatin, the force on an atom is only large if

$$|2(\delta - \mathbf{k}\cdot\mathbf{v})| \lesssim \Gamma\sqrt{1 + I/I_0}.$$

Thus atoms much outside a certain velocity range will experience little damping, and aomts initially within this range will be decelerated out of it. Only a small portion of the total velocity distribution has been decelerated by only a small amount. One way to solve this problem is Zeeman tuning (or Zeeman slowing) [6] where a spatially varying magnetic field compensates the changing Doppler shift as the atoms decelerate so as to keep the atoms near resonance.

Our lab uses several laser beams to decelerate the Strontium atoms and use a Zeeman magnetic field to keep the atoms in resonance with the laser.

1.2 The use of a 689nm Laser in Strontium Atomic Transitions

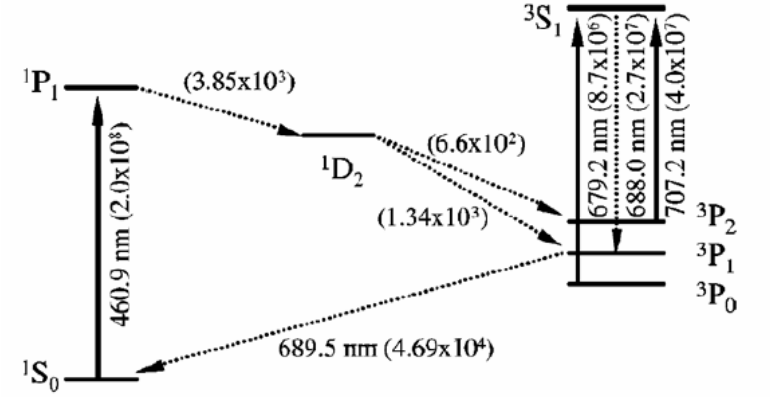

Figure 1. Partial Strontium Energy Level Diagram. The cycling transition between $^1S_0$ and $^1P_1$ has a sub-transition from $^1S_0$ to $^3P_1$,with a wavelength of 689.5 nm [6].

Strontium atoms experience cycling transition between $^1S_0$ and $^1P_1$states, with a wavelength of 461nm [6]. One of the sub-transition involved in this cycle is from$^1S_0$ to $^3P_1$, with a wavelength of 689nm, as shown in figure 1. The scattering rate of this narrow transition is just large enough to make it feasible to trap atoms using the techniques described above. Therefore, a Doppler cooling mechanism operating on this transition can capture atoms that have been pre-cooled on the 461mm transition. In our experimental set-up, laser beams of wavelengths 461nm and 689nm are produced and split into six orthogonal laser beams to slow down the atomic sample from all directions, as shown in figure 2 [7].

In one word, the purpose of this project is to build and characterize a 689nm laser to be used in a Doppler cooling mechanism on the $^1S_0 \rightarrow {}^3P_1$ transition of Strontium atoms, which serves as part of a cooling and trapping system to produce dense, ultracold atomic samples.

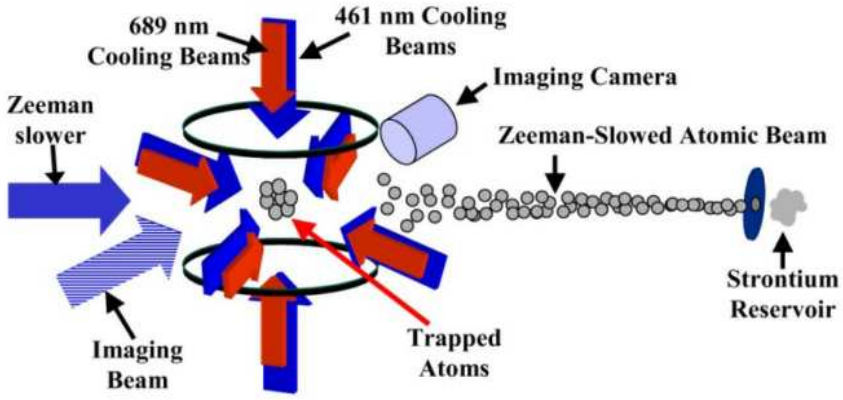

Figure 2. The overall set-up of the Magneto-Optical Trap[7]. Six 461nm and 689 nm beams (red and blue arrows) each shines from six orthogonal directions to slow down the Strontium atoms at the center (grey). The atoms are loaded from a Zeeman-slowed atomic beam.

1.3 Laser Background

To introduce the concepts that are important for understanding the properties of the diode laser being built in this project, we start by describing how lasers work in general and how diode lasers work.

Laser operation is based on stimulated emission, the phenomenon that an atom in an excited state ΔE above the ground state can absorb a photon of energy ΔE, then immediately emitted two identical photons of energy ΔE and thus jump back to the ground state. In a laser, there is a gain medium in which a significant portion of the atoms are somehow pumped to an excited state and photons with the corresponding frequency are directed to these excited atoms to start a stimulated emission. Every two photons emitted from an atom jumping down to ground state will each start more simulated emissions for more atoms, as long as there are more atoms available on the excited state. As a result, a large number of photons produced from stimulated emissions come out of the gain medium as the output of the laser. There needs to be a pumping power strong enough to make sure that there is always sufficient number of atoms in the excited states. The stronger the pumping power, the more stimulated emission can occur, the stronger the output beam is and the higher the gain is. There is a threshold, called the "laser threshold", which is the minimum pumping power to enable just enough stimulated emissions to keep the laser operate. In this case, the photons produced are just enough to compensate for those going out of the gain medium, for which the gain of the laser is unity.

We chose to build the laser from a semiconductor laser diode because they are cheap, simple, and can reach a laser power of a few milliwatts, which is sufficient for our cooling system. However, instead of building a laser from a bare diode, we chose to add an extended cavity to the diode. To understand why this is the case, we should first describe the properties of a laser formed only by a bare diode, and discuss its limitations.

For a diode laser, the gain medium is a semiconductor lattice, and the pumping power is the current. The "laser threshold" for a diode laser, therefore, is a minimum current to make the diode lase, which is called the "threshold current" of the diode laser. Since the higher energy levels of semiconductors come in bands, the atoms can be pumped into many different energy levels, each of which gives a photon of a different frequency when it jumps down to the ground state. As a result, the output photons can have a mixture many frequencies and is thus highly multimode.

Since many applications of lasers require specific frequencies, an internal cavity is added to a diode laser to allow frequency selection. The cavity is formed by two parallel reflectors, such as mirrors, that are facing each other and spaced by a certain distance. One of the reflectors allows small transmission of light. As light gets reflected back and forth between the reflectors, most frequencies die out because of destructive interference, and only frequencies that can form a standing wave in the cavity can interfere constructively and therefore get transmitted. This cavity, because of its plane, parallel reflectors, can be characterized as a Fabry-Perot cavity [8]. The cavity of a diode laser is the facets of the semiconductor lattice.

Since there are infinitely many equally spaced frequencies in resonance with the cavity, the amplitude vs. frequency curve has a close-to-zero ground and equally spaced peaks. The spacing, in Hz, of the resonance frequencies is called the free spectral range (FSR) of the cavity, given by

$$\Delta\nu = \frac{c}{2nL}$$

where c is the speed of light, n the index of refraction of the diode medium, and L the length of the cavity.

As discussed earlier, the gain of a laser is determined by the pumping power, which, in the case of diode lasers, is the driving current. The amplitude vs. frequency curve for a certain current value above the threshold current is a smooth curve covering a wide range of frequencies. For a fixed temperature, the gain from the diode medium and the frequency selection of the diode cavity combine to give an overall gain of the diode, as shown in figure 3[3].

Since the smooth medium gain curve does not select certain cavity transmission peaks over the others, there are several peaks competing to dominate, thus the output light tends to be unstable and multimode. These properties make it very important to introduce a mechanism for controlling the wavelength of the laser.

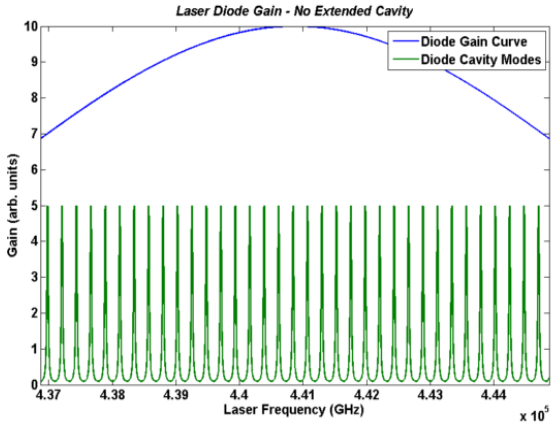

Fig. 3: Bare laser diode without an external feedback element. The laser diode's gain curve (blue) is divided into allowed regions by the allowed modes of the laser diode (green). Since the modes are so closely spaced, the laser diode easily switches between them and has trouble achieving single-mode operation [3].

Many different approaches have been made to build a system in which a diode laser can operate in a stable, tunable, single-mode fashion. One approach is to put in some other frequency-selective tools that have a much narrower selection range, so that the gain curve can select a dominant frequency more easily. This is how External Cavity Diode Lasers come into play.

1.4 Extended Cavity Diode Laser (ECDL)

The laser being made in this project is an Extended Cavity Diode Laser that is expected to allow stable, single-mode operations. An Extended Cavity Diode Laser (ECDL) is a system in which an external component is added to the laser that feeds back laser light to the diode. These photons get fed back into the gain medium initiate more stimulated emissions of a certain frequency. Thus an optical feedback increases the gain of the diode laser. Only frequencies allowed by both the internal cavity of the diode and the added external cavity can propagate, thus the transmission curve of the ECDL system has much fewer significant peaks than that of a naked diode. By properly tuning the extended cavity, one can select a dominant output frequency and therefore makes the laser single-mode and much more stable.

The heart of an external cavity is the diffraction grating, an optical instrument that diffract incident light into different directions according to the frequency of the light, according to the grating equation [9]

$$n\lambda=d[\sin(\theta_i)+\sin(\theta_d)]$$

where d is the spacing of the grating grooves, n is a non-negative integer, λ is the wavelength of the incident light, θ_i is the angle of incidence, and θ_d is the angle of diffracted light measured from the

opposite side from that of the incident beam. This is illustrated in figure 4. The diffracted beam for which n=0 is called the zeroth order diffracted beam. We see that in this case b=a, so the zeroth order diffracted beam is simply the reflected beam, independent of the wavelength. The diffracted beam with n=1 is called the first order diffracted beam, for which b is a function of λ.

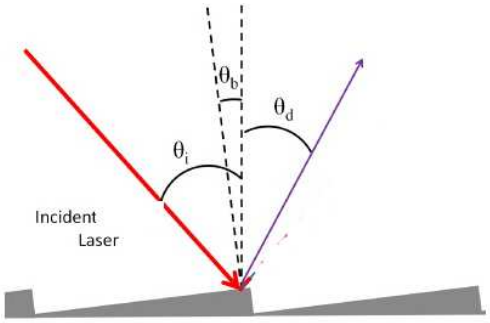

Figure x. The optical path of a ray passing through a grating. Note that the angles are measured from the grating normal, not the facet normal.

The most common ECDL configurations are Littman-Metcalf and Littrow cavity lasers, which both make use of diffraction gratings. These configurations are shown in figure 5. In the Littrow configuration, the grating is aligned such that the first order diffraction returns directly to the laser diode as the optical feedback. By varying the relative angle of the diode face and the grating, one can tune the frequency of the feedback and therefore tune the dominant output frequency. Due to the simplicity of this configuration, the output power, which is the zeroth order reflected beam, can be as high as 80% of the diode output, which is an advantage because a feedback with higher power can take better control of the internal cavity of the diode and hence enable more sufficient frequency tuning. However, the angle of the output beam changes slightly as the angle of the grating changes, which makes the next-stage alignment of the output beam difficult.

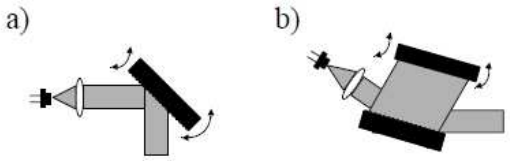

Figure 5. ECDL configurations. a) In the Littrow configuration, up to 80% of the power is coupled out. b) In the Littman-Metcalf configuration, the output beam does not wander as the wavelength changes. [2].

In the Littman-Metcalf configuration, on the other hand, the first order diffracted beam is sent to a mirror which reflects the beam back on the grating and then to the diode. Frequency tuning is then

accomplished by varying the angle of the mirror, which changes the frequency of the light fed back to the grating. Since the grating does not move, the output zeroth order beam does not change direction as the frequency is tuned, which is an advantage. This configuration was first used in 1978 by Littman and Metcalf, who built a dye laser with a spectral half width of 1.25GHz and a peak power of 10kW at 600nm [10]. The disadvantage of Littman-Metcalf configuration is that it gives lower output power because the feedback is a twice-diffracted beam and thus a larger fraction of the power must be diffracted to give enough feedback.

We decide to use the Littman-Metcalf configuration because we value the spatial stability of the zeroth order output beam, which is an important for the creation of six orthogonal beams.

2. Design and Construction

2.1 Overall Optical Path of the System

The configuration of this Extended Cavity Diode Laser with Littman-Metcalf configuration is shown in figure 6. The detailed mechanical drawings of the self-fabricated optical mounts are listed in Appendix 1. The output beam from the diode is collimated by a lens located immediately next to the diode. the collimated beam then hits a diffraction grating. The zeroth order reflected beam serves as the output of the ECDL. The first order diffracted beam is reflected by a mirror and then coupled back into the diode. By varying the relative angle of the mirror and the grating, one can tune the frequency of light being fed back to the diode and therefore tune the dominant frequency of the output.

2.2 Aligning and Tuning of Extended Cavity

Such tuning is accomplished by a leverage associated with the optical mount of the mirror. The mirror is mounted at the end of the long arm of a pivoted L-shaped piece. A commercial Piezo-electric Transducer (PZT) from Thorlabs (Part #: AE0203D04F) is glued to the long arm. Varying PZT voltage moves the arm of the L-shaped mirror mount and hence moves the mirror. This changes the relative angle between the mirror mount and the grating and therefore enables fine tuning of the ECDL.

It is important to do some coarse alignment before the fine PZT tuning, to make sure that the feedback beam falls safely on the diode surface without missing it entirely. The system is so sensitive that a little drift of the environment will slightly change the optical path and deviate the feedback beam from

hitting the diode surface. Therefore, a coarse alignment needs to be made over a certain period of time, usually once a day.

Such coarse alignment is done manually using two fine screws. The screw behind the PZT push the mirror mount to a reasonable starting position before the PZT adjust it over a much smaller range. The screw can move the mirror mount within a 3-5mm range, but one must be cautious not to crush the PZT by pushing the screw too hard. The fine screw behind the grating

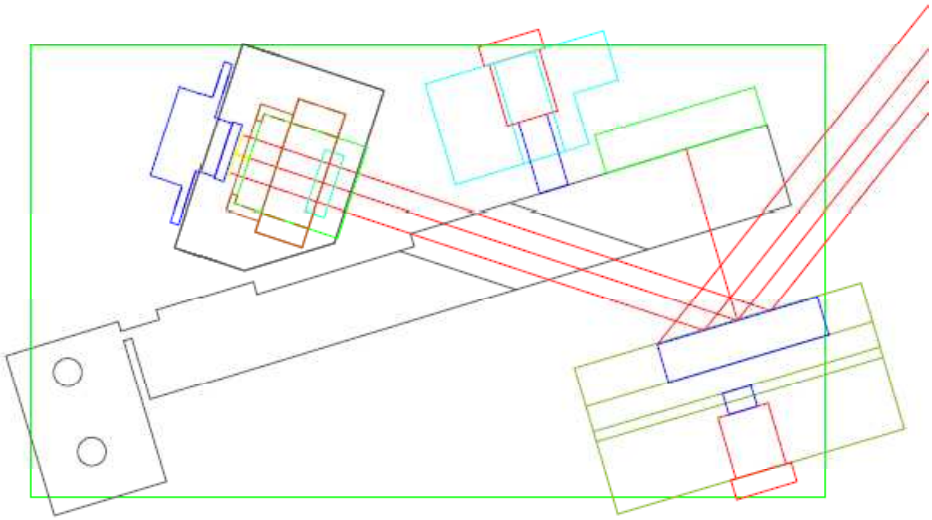

Figure 6. The overall configuration of the ECDL. The path of the beams are indicated by red lines. A diode laser on the upper left corner (blue) produces a raw laser beam, which is immediate collimated by a collimating lens (red) held by the same optical mount (green). The collimated beam passes a hole of the L-shaped mirror mount and reaches the diffraction grating (blue) on the lower right corner. The zero-order reflection comes out of the system, but the first-order diffraction is reflected by the mirror (green) and then coupled back to the diode. Two PZT's (pink) are placed toward the L-shaped mount to adjust its position.

holder, on the other hand, pushes the grating back and forth within an approximately 3 mm range. By playing with the two fine screws, one can make sure the feedback safely hits the diode surface. In particular, one can lower the driving current to the threshold current of the naked diode and manually adjust the two screws until seeing a dramatic output power increases. This is because the diode will have a greater gain when it receives an external feedback, and therefore experience a power increase. Near the threshold current, this increase is the most dramatic, usually up to 100% ~200%.

2.3 Stabilize the ECDL System

Although the ECDL system is highly sensitive to drifts of the environment, effort has been made to minimize such influence. To minimize mechanical vibrations, all optics are mounted to holders made of brass or stainless steel. These holders are screwed to a brass base fixed on top of a thick aluminum bulk, which is anchored onto a vibration-proof optical table. Such design is to minimize the vulnerability of the ECDL optical path to external vibrations.

Apart from mechanical vibrations, temperature fluctuations can also affect the behavior the of the ECDL by affecting the index of refraction of the diode gain medium. They also cause expansion and contraction of the optical mounts and therefore change the optical path. To minimize such fluctuations, the temperature of the ECDL is set and maintained by a commercial temperature control unit (Wavelength Electronics HTCEVALPCB), which use a thermistor (Thorlabs TH10K) and a thermo-electronic cooler (Marlow RC12-8-01L). Moreover, the aluminum bulk acts as a large heat-sink that keeps the temperature stable over long periods of time. Such control of mechanical and thermal fluctuations can significantly reduce the drift of the ECDL to the order of 0.01 cm^{-1}/h, which is sufficiently small for our purpose [2].

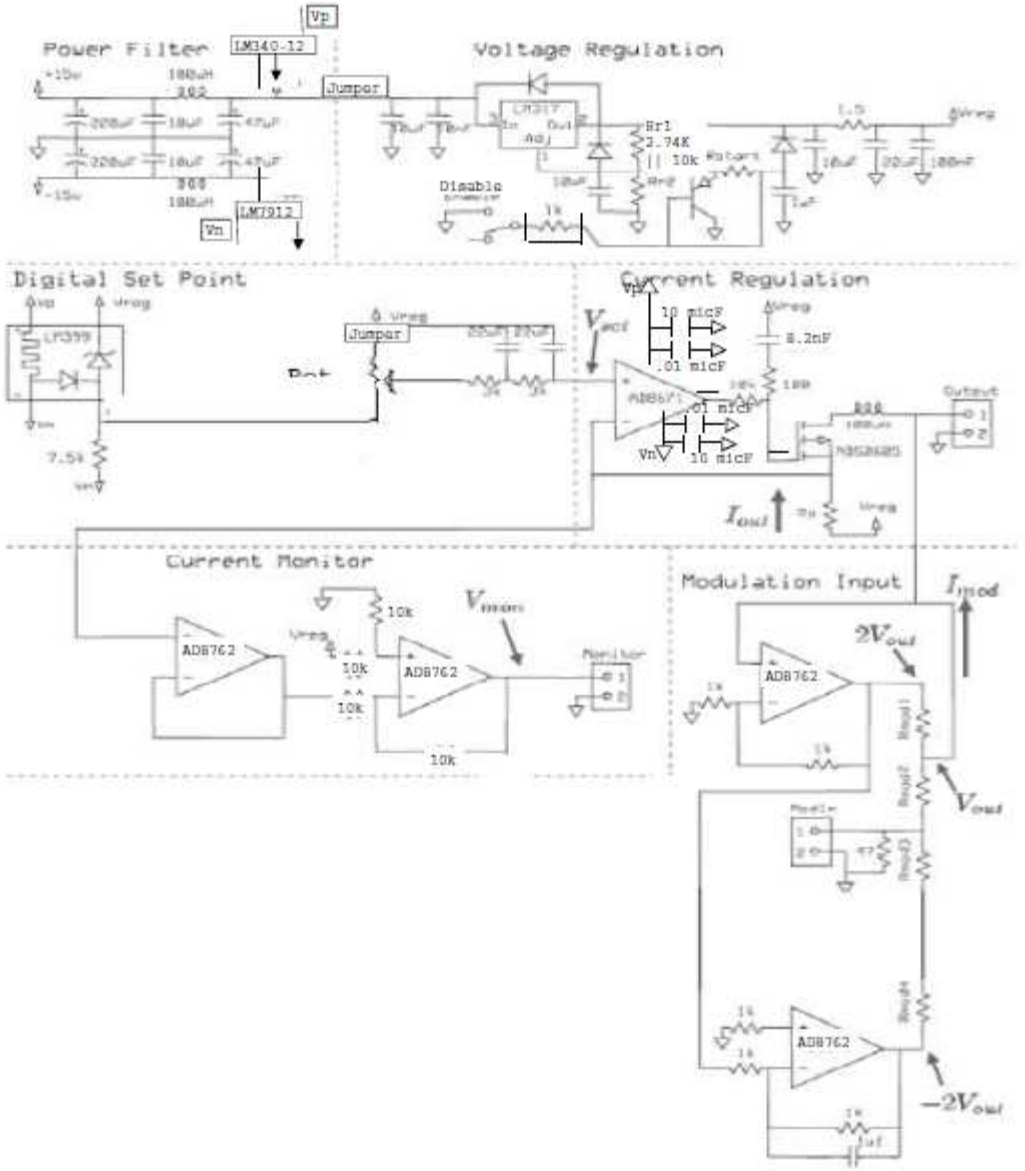

Figure 7. The schematic design of the current driver circuit. The voltage across the diode is set by a extremely stable voltage reference generated by V_{reg} in the voltage regulation sub-circuit and the Voltage drop across the LM317 at the "set point" sub-circuit. Once the diode voltage is set, the current is regulated to remarkable stability by the current regulation circuit, which can be checked by current monitor.

2.4 A Current Driver Circuit for the ECDL

Due to the high stability requirements of laser optics, few commercial current drivers are too noisy to supply the laser diode. Therefore, a current driver circuit must be made to supply stable current. We adapt a current driver design from Ref.11 and modified it. The major change we made was to replace the digital set point in the original circuit by an analog set point. The schematic of our circuit is shown in figure 7. The part numbers of the elements in the circuit are listed in Appendix 2.

The "power filter" and "voltage regulation" sub-circuits, power lines are first filtered by a series of capacitors and inductors to provide ±12V voltage supply to power all op-amps in the circuit. The filtered power is then regulated with the LM317 adjustable voltage regulator to generate the extremely stable regulation voltage (V_{reg}). This voltage is used to drive current to the laser diode in the "current regulation" sub-circuit and to generate set-point voltage in the "set point" sub-circuit. The "current monitor" sub-circuit generates a voltage proportional to the output current of the driver so that the output can be monitored.

The current sent to the diode can be determined by measuring the monitor voltage of the circuit, which is directly proportional to the output current, with a ratio that can be easily determined by a calibration. To calibrate, the circuit was isolated from the diode, and the output was connected to a "dummy diode", a diode in series with a resistor with a known resistance, usually around 10 ohms, which is similar to the resistance of a diode. By measuring the voltage across the resistor as a function of the monitor voltage, it is easy to find the relationship between the output current and the monitor voltage.

It is worth noting that the measured output voltage must be the voltage across the resistor, instead of the voltage across the entire dummy diode. Another remark is that technically, we should obtain the same calibration results if the output is connected to the resistor alone. However, a diode connected in series with the resistor can better simulate the real situation.

The calibration was carried out using a resistor with R_{cal}= 10Ω. The voltage drop across the resistor was measured for several different monitor voltage values, and they form a linear relationship with a slope of 0.1977, as shown in figure 8.

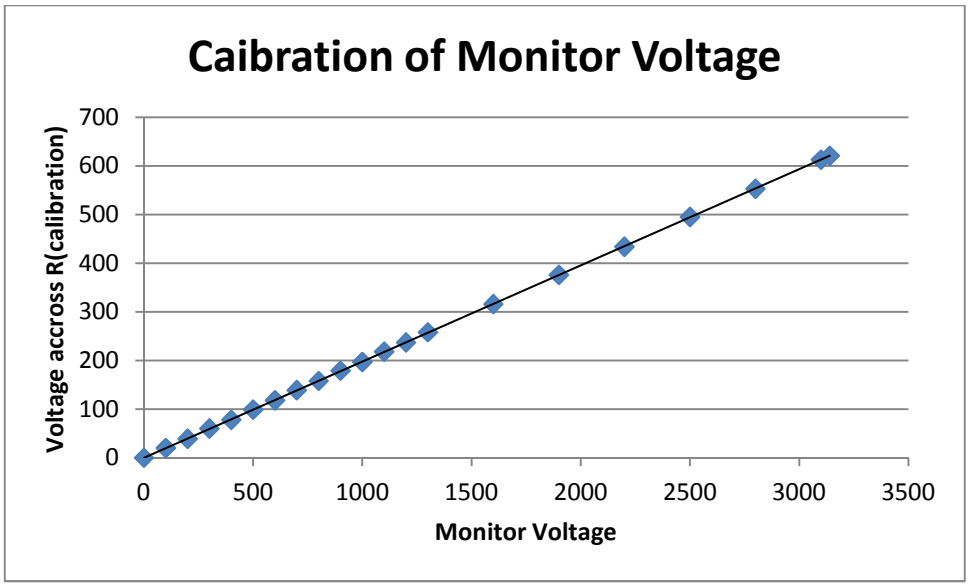

Figure 8. The calibration of monitor voltage. A linear relationship $V_{cal}=0.1977V_{mon}$ is seen from the data points.

Therefore, the output current, which is the current across R_{cal}, is $I_{out}=V_{cal}/R_{cal}=V_{cal}/10\Omega$. Therefore, the output current can be determined by measuring the monitor voltage by

$$I_{out}=V_{mon}*(V_{cal}/V_{mon})/R_{cal}=0.1977/10*\ V_{mon}=0.01977\ V_{mon}$$

Therefore, during the characterization of the laser, we can characterize the driving current of the laser by measuring the monitor voltage.

3. Threshold and Power

3.1 Threshold Current

One of the most important characteristics of a diode laser is its threshold current, the current at which the density of electrons and holds is high enough that the gain of the laser is greater than 1, or the current at which an emitted photons is more likely to create stimulated emission than to get absorbed. An ECDL system is expected to have a lower threshold current than the bare diode because the photons fed back to the diode from the extended cavity are reflected into the gain medium and thus induce more emissions. Therefore, a current that is not enough to cause stimulated emission in a naked diode may be able to cause stimulated emission in the ECDL because more photons are involved.

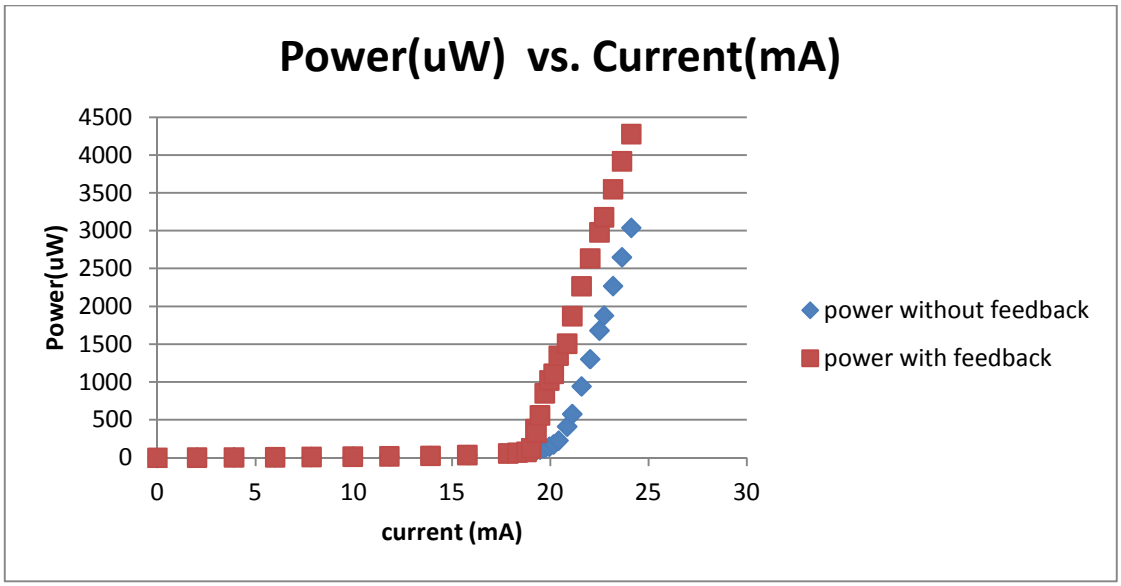

Figure 9. Laser threshold with (red) and without (blue) external cavity feedback. The laser power is normalized to an arbitrary scale to show the threshold location more clearly. One can see that the laser threshold is lowered by the feedback.

Figure 9 shows the thresholds of the bare laser diode and the ECDL. The laser current was increased in small steps by manual adjustment of the variable resistor in the current driver circuit. The output laser light is recorded on a powermeter, a digital device that displays the power of a light beam. From the figure, it is then clear that the threshold current is lower for the ECDL, as expected. In fact, the measured threshold current of the bare diode is 19.9mA, and that of the ECDL is 19.0mA, which indicates a noticeable decrease of threshold current when using an extended cavity.

3.2 Output Power

Apart from the threshold current, another important characteristic of a laser is its output power above the threshold current. The power of a diode is expected to increase linearly with driving current above the threshold. Adding an extended cavity to the system should not change this behavior. Figure x shows the laser power as a function of the applied laser current, which is a line with a slope 0.794mW/mA, in agreement with the expectation of a linear relationship.

Although the bare diode was rated to 35 mW of total output power, we start to see abnormities when the output power exceeds 7mW. One possible cause of these abnormities is that the operating power limit for an ECDL is much lower than that of the bare diode. Since the light coming out of the diode is reflected and diffracted several times in the extended cavity, the resulting amount of power within the internal cavity of the diode can be very high even for relatively low ECDL output power. Such high power in the internal cavity may exceed the diode's ratings and cause problems. Fortunately, since the output power needed for our laser cooling experiment is no more than 2 or 3 miliwatts, the power of the ECDL is sufficient before any abnormity occurs.

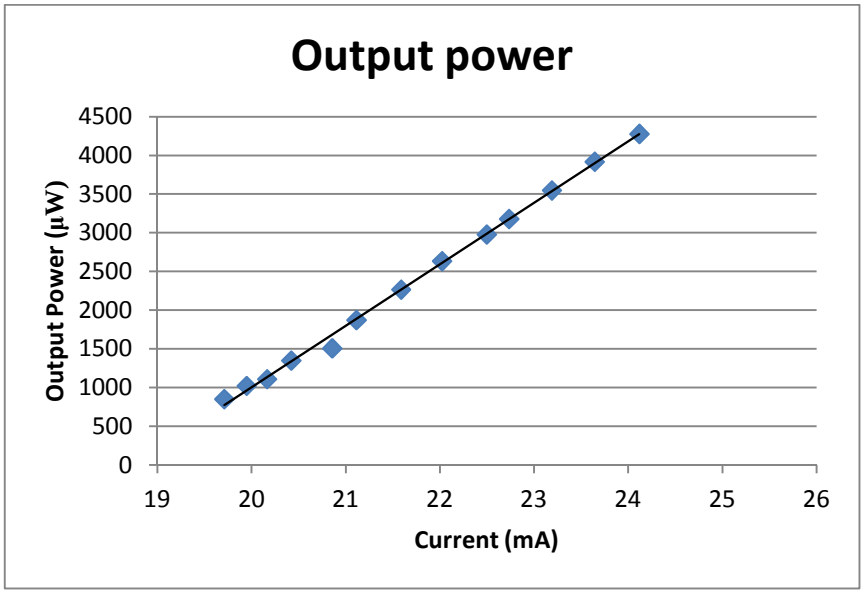

Figure 10. Laser power from threshold is linear with a slope of 794µW/mA, i.e. 0.794mW/mA.

3.3 Choice of Diffraction Grating

Apart from the output power, it is also interesting to study the power of the feedback the extended cavity sends to the diode. As mentioned before, the Littman-Metcalf ECDL configuration does not give very strong feedback, but we need the feedback beam to be as strong as possible because a feedback with higher power can take better control of the internal cavity of the diode and hence enable more sufficient frequency tuning.

As explained in section 1.4, the first order diffraction of the diode output beam hits the mirror, gets reflected back to the grating, and then to the diode. Thus stronger first order diffraction from the grating will results in stronger feedback. One important parameter of the grating that affects the intensity of first order diffraction is its density of grooves. Gratings with fewer grooves per unit length are expected to diffract a larger fraction of incident light to the first order than gratings with denser grooves do. However, this is just an overall trend. The actual behavior of the grating depends largely on the wavelength of the light and the angle of incidence. The downside of gratings with fewer grooves, on the other hand, is resolution. When used in the laser cooling experiment, the output beam of this ECDL is expected to have a beam waist of a few hundreds of microns. Therefore, it is important to have reasonably good resolution from the diffraction grating.

To negotiate between resolution and first order power, we installed three gratings with different groove densities to our ECDL system one at a time and compared their behaviors. We used commercial gratings from Thorlabs: a 1800 grooves/mm ruled grating, a 1200 grooves/mm ruled grating and a 1200 grooves/mm holographic grating. The resolutions of these gratings are all sufficient for our experiments. And according to their power ratings from the manufacturer, these three gratings have relatively strong first-order diffraction at the wavelength 689nm compared to most other gratings.

We positioned each of the three gratings with the diode as in the actual set-up, remove the mirror, and use a powermeter to record the power of different diffracted beams. The results are shown in table 1.

Grating Type with part #	Total incident power from the diode (mW)	Zeroth order reflection (mW)	First order diffraction (mW)	Second Order Diffraction (mW)
1800g/mm, Holographic (Thorlabs GH25-18V)	211	152	33	Not detectable
1200g/mm, Ruled (Thorlabs Gr25-1208)	211	85	30	30

1200g/mm, holographic (Thorlabs GH25-12V)	211	150	30	10

Table 1. The power of diffracted beams for different gratings. The 1200g/mm gratings have similar levels of first order feedback to the 1800g/mm grating, which is not expected.

These results disagree with the expectation that the 1200g/mm grating will have a stronger first order diffracted beam. All three gratings gives very similar amount of first order feedback and no advantages are observed for either of the 1200g/mm gratings. In conclusion, we chose the 1800g/mm ruled grating, which has the same level of first order diffraction power and better resolution compared to the1200g/mm ones.

4. Characterization Techniques

The laser was designed with the intention of using the diode current, the PZT voltage and the temperature of the system as the main means of frequency tuning. The frequency decreases when the temperature increases, or when the current increases, and it is also extremely sensitive to the optical feedback provided by the extended cavity. However, there are not linear smooth tunings but are subjected to mode hops. We therefore wish to characterize all of these mechanisms, so that we could find the laser's mode-hop-free tuning range when each of these tuning parameters was employed. We were also interested in the slope of the linear dependence of the wavelength on each of these parameters. Since PZT tuning will be the most efficient tuning method for tuning in short timescales, we would attempt to find an optimized combination of temperature, current and a starting point of PZT voltage that gives the maximum mode-hop-free PZT tuning range.

Two major equipments are used to measure the mode-hop-free tuning range of the laser: a Fabry-Perot interferometer and a wavemeter.

4.1 Fabry-Perot Interferometer

The Fabry-Perot interferometer is a cavity that works the same way as a laser diode internal cavity does. Like the two mirrors at both ends of a diode, a Fabry-Perot interferometer consists of two partially reflecting, curved surfaces, as shown in figure 11. Light transmits through the cavity only when the cavity size is such that the light interferes constructively in the cavity. The length of the cavity is coarsely tuned using a thread on the locks holding the mirrors. The output coupler mirror is mounted onto a large stack PZT, which enables fine tuning of the cavity length.

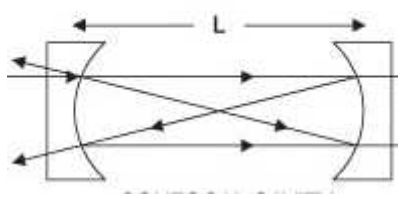

Figure 11. The diagram for a Fabry-Perot cavity. Light from the left gets reflected back and forth in the cavity, and a small part gets transmitted to the right as the output. Since only the light with frequencies in resonance with the cavity interferes constructively after several reflections, they dominant the output.

Similar to the diode internal cavity discussed in Chapter 1, there are infinitely many equally spaced frequencies in resonance with the cavity, The free spectral range (FSR) of a Fabry-Perot cavity, which is the spacing of resonance frequencies, is given by

$$\Delta\nu = \frac{c}{2nL}$$

where c is the speed of light, n the index of refraction of the cavity medium (air, in our case), and L the length of the cavity. The Fabry-Perot cavity used in this project has an FSR of 500MHz.

For a laser beam with a specific frequency (f), it is usually unlikely that this frequency will exactly be in resonance with the cavity and therefore gets transmitted through. Therefore, in most times no signal is seen from the cavity output. However, if we continually ramp the cavity length (L) over a range that is larger than its FSR, there must be a set of L values over this ramping range which are in resonance with f. Therefore, if we drive the PZT attached to the Fabry-Perot cavity by a triangular wave and use it to ramp the cavity length, we will see no output signal when the L value does not match f, but a strong signal when it does. Thus the resulting transmission vs. frequency function will have a low ground and many equally spaced peaks. As the laser frequency changes, a different set of L values will be in resonance with the new frequency and thus the peaks shift.

Since the length of our Fabry-Perot cavity is more than 10 centimeters, it is a challenge to line up the input beam exactly with the cavity axis. However, this collimation can be much easier if the Fabry-Perot cavity is made confocal, meaning that each curved mirror is at the other's focal point [12]. In this case, even beams that are not very well lined-up with the cavity axis can pass through because they will become parallel to the cavity axis after being reflected back and forth in the cavity for a few times.

It is difficult to adjust the cavity to the confocal position just by measuring the cavity length. Instead, we first send in a calibration beam attached to the cavity that was precisely lined up with the cavity. We then manually tuned the cavity length by carefully moving the tuning thread when the cavity was ramped by a PZT. The peaks of the transmission vs. frequency function are the highest and narrowest when the cavity is confocal, and become broad and low as L moves away from it. In this way, the confocal position can be constructed and the alignment of other beams becomes much easier.

In one word, by coupling the (presumably single-frequency) ECDL output into a Fabry-Perot cavity and ramping the cavity length using the PZT, we can find, for this specific frequency, the cavity transmission as a function of cavity length, which should be a flat line with peaks equally spaced by FSR. When frequency of light changes, the locations of the peaks will shift but the spacing remains unchanged.

For mode-hop free tuning, the peaks shift linearly with frequency. This linear relationship makes it very easy to experimentally tune the laser frequency by inspecting the relative position of the transition peaks. However, this linear relationship usually does not go over all frequencies due to the restrictions set

by the geometry of the ECDL. Clearly, a longer mode-hop free range is experimentally more desired than a shorter mode-hop free range. Therefore, the mode-hope-free frequency ranges for each tuning parameter are an important character of the ECDL.

4.2Wavemeter

Part of the output of the ECDL was coupled into the sensor of a wavemeter, a digital device that displays the wavelength or frequency of laser light input into the wavemeter. A wavemeter has the advantage over the Fabry-Perot interferometer that it gives the absolute wavelength, whereas the Fabry-Perot interferometer only gives relative comparisons of different frequencies and thus can be useful only with continuous tuning over a large frequency range. The disadvantage of a wavemeter is that its response time is much slower than that of the interferometer, and it does not tell whether the light is single-mode. Moreover, it does not reach the level of precision needed in this experiment (at least on the order of 10 MHz), which the analog signal provided by the Fabry-Perot cavity will do. A wavemeter is very useful in conjunction with the Fabry-Perot interferometer to both qualitatively and quantitatively study the behavior of the ECDL.

4.3 Overall Setup

The overall experimental setup for the ECDL characterization is shown in figure 12. The output of the laser was passed through a beam splitter that reflects a small fraction of incident light. The reflected light was coupled into the sensor of a wavemeter using two mirrors. The transmitted light was rotated by 90^{o} using a beam rotator and then coupled a Fabry-Perot interferometer using a mirror and a beam splitter. The output of the Fabry-Perot cavity was detected by a photodiode. All optical instruments are mounted on commercial kinematic mounts from Thorlabs which allow fine adjustments of the mounting angles.

Not shown on the diagram are the current driver circuit and the TEC control circuit, which are each put in a aluminum box to avoid electrostatic damage. The two PZT each driving the ECDL mirror mount and the Fabry-Perot cavity respectively, are connected to a PZT controller module which is driven by a function generator. The photodiode is connected to a digital oscilloscope to display the cavity transmission signals.

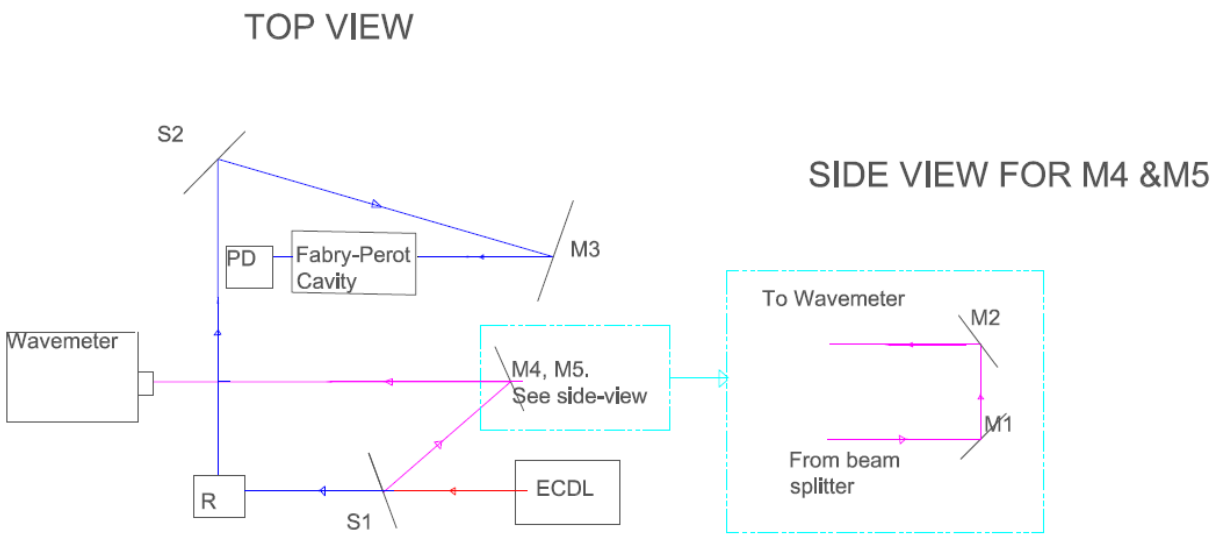

Figure 12. The overall set-up of the ECDL characterization. The light comes out of the ECDL and is coupled into a wavemeter and a Fabry-Perot cavity. M's are mirrors, S's are beam splitters, R is the beam rotator, PD is the photodiode. The sensor of the wavemeter is higher than the optical plane, so two mirrors, M1 and M2, are used to send the beam up to the level of the wavemeter sensor, as shown in the side view.

5. Mode-hop-free Tuning Range Characterization

As discussed in the previous chapter, an important characterization of the laser is its mode-hop-free frequency tuning range when the temperature, current or the length of the extended cavity is being varied. Unfortunately, due to the limit of time, we have so far only characterized the current and cavity length.

As described in Chapter 2, the PZT on the mirror mount of the ECDL enables fine tuning of the length of the extended cavity. Within the mode-hop free tuning range, each PZT voltage value allows a specific frequency to be fed back to the diode and therefore dominate the output frequency. The Fabry-Perot cavity gives a transmission curve for each PZT voltage, which has many peaks equally spaced by FSR of the cavity. For different PZT voltages, the positions of peaks on the transmission curve are different. Within a mode-hop-free range, the laser frequency should change linearly with the mirror mount PZT voltage, and so do the peaks of the transmission curve. Therefore, by plotting transmission curves for several equally spaced PZT voltage values, one can see the peaks shift by an equal amount for each PZT voltage spacing. For mode hops, the peak shifts does not have such regular patterns. In this way, the mod-hop-free range of the laser can be graphically determined.

In this project, the PZT being used allows a voltage tuning range 0~150V. The mode-hop-free tuning range is on the order of a few volts.

5.1 Calibration

The FSR of the Fabry-Perot cavity used in this experiment is claimed to be 500MHz. The cavity was calibrated to verify that this is indeed the case. In the calibration, the mirror mount PZT was set to several different voltage values. For each voltage value, the output light is sent into both the Fabry-Perot cavity and the wavemeter. By observing the transmission curves and the measured laser frequency, one can calculate the frequency change when the peaks have shifted for one spacing period. Since the transmission curve spacing equals the FSR of the Fabry-Perot cavity, the frequency change over the spacing calculated from the wavemeter readings is the actual FSR.

Figure 13 (a) shows the transmission curves for different PZT voltages ranging from 21.9V to 31.4V at steps of 0.4V. To eliminate other variables, the current and temperature were set to be fixed. T=21.50^{o}C and I=25.820mA. From the plot, the mode-hop-free range starts at the third curve from the bottom and ends at the ninth curve from the top, because the frequency changes linearly within this range and this linear pattern stops out of this range. It can then be observed that over this mode-hop-free range, each peak has shifted for a total of approximately two spacings. The frequency change over this range can then

be determined by the frequency, measured by the wavemeter, for each PZT voltage, as plotted in figure 13(b). It can be observed that the frequency change over the mode-hop-free tuning range is approximately 1.0 GHz.

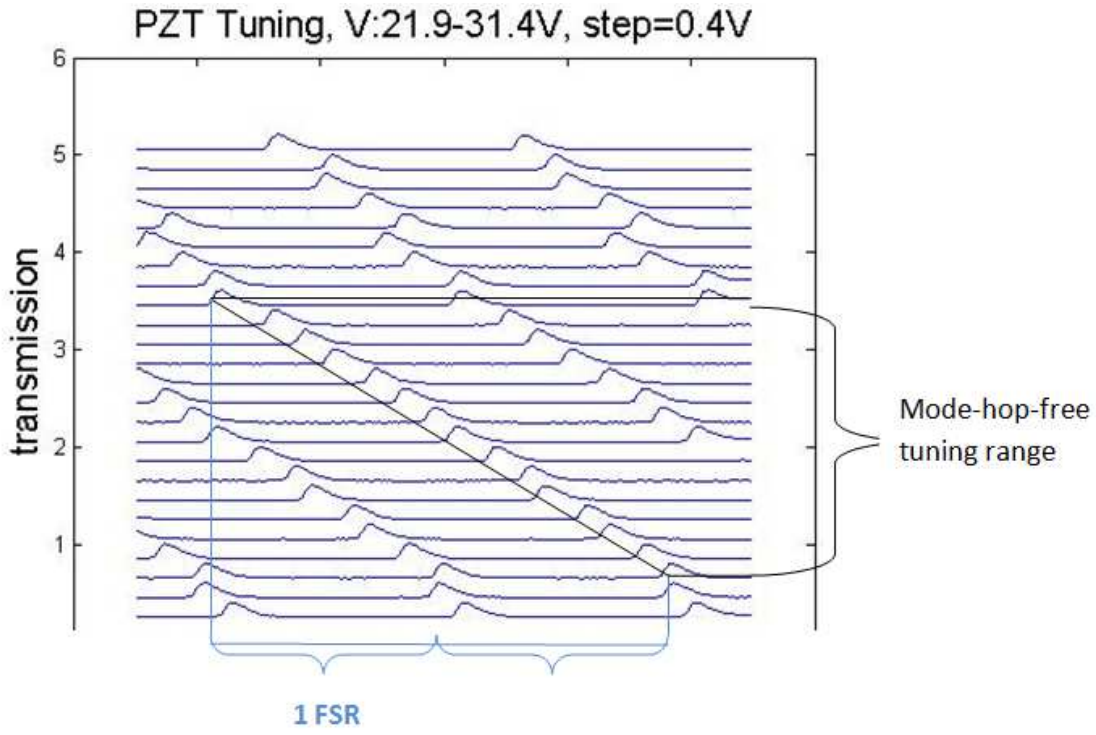
PZT Tuning, V:21.9-31.4V, step=0.4V
transmission
6
5
4
3
2
1
Mode-hop-free
tuning range
1 FSR

(a)

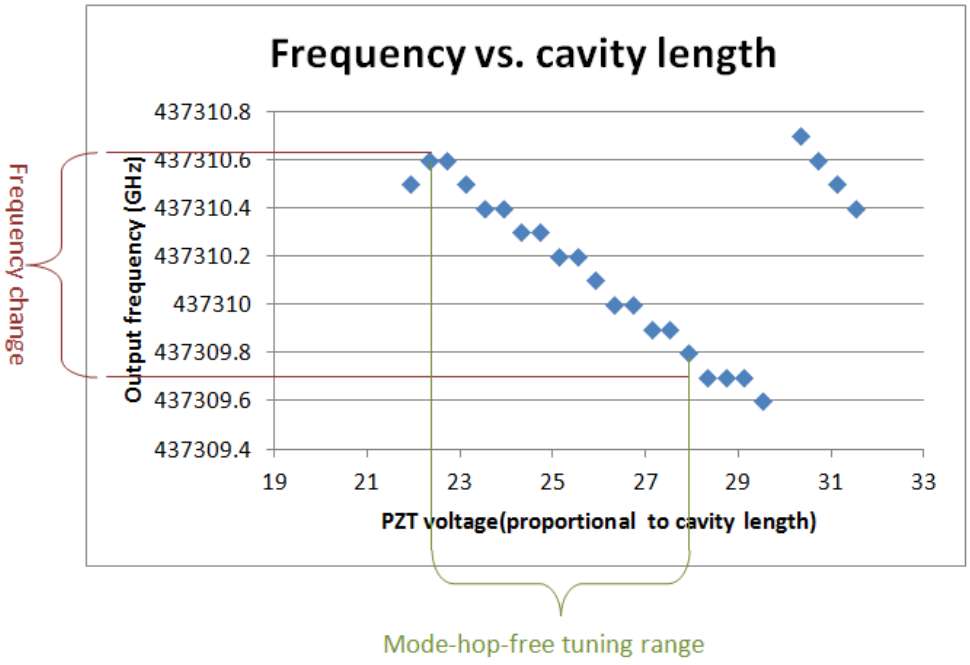
Frequency vs. cavity length
Output frequency (GHz)
437310.8
437310.6
437310.4
437310.2
437310
437309.8
437309.6
437309.4
19
21
23
25
27
29
31
33
PZT voltage(proportional to cavity length)
Frequency change
Mode-hop-free tuning range

(b)

Figure 13. Calibration of the Fabry-Perot cavity with fixed current I_1=25.820mA and temperature T=21.50^{o}C.

(a) shows a mode-hop-free range of the PZT tuning (black brackets), for which the transmission peaks shift linearly with the voltage over the entire range (as indicated by the linear fit). The x-axis of the plot is simply the time associated with the ramping of the PZT voltage. Each peak has shifted for approximately two FSR's over the mode-hop-free range (blue brackets).

(b) shows the change of frequency (brown brackets) over this mode-hop-free PZT tuning range (green brackets). The frequency has changed for approximately 1.0GHz.

From the data, the frequency has changed for approximately 1 GHz for 2 free spectral ranges (FSR), which indicate each FSR to be 500MHz, as claimed by the manufacturer. Therefore, the calibration shows that the actual FSR of the Fabry-Perot cavity is in very good agreement with the claimed value, 500MHz.

5.2 PZT Tuning Characterization for Different Current Values

As stated in the beginning of the chapter, the mode-hop-free range of the PZT on the ECDL mirror mount can be graphically determined by comparing the transmission curves for equally spaced PZT voltage values. In this way we can find the mode-hop-free tuning range in terms of PZT voltage and the corresponding frequency tuning range. To characterize this linear relationship between frequency and PZT voltage, which is an important feature of mode-hop-free tuning, we wish to find the slope df/dV. Moreover, as mentioned in Chapter 1, this laser is to provide 689.5nm laser beams as part of laser-cooling mechanism for Strontium atoms. Therefore, it is important to check if this wavelength can indeed be reached during the mode-hop-free tuning processes.

We start with performing these characterizations to our calibration data, which includes a mode-hop-free tuning range. The whole set of calibration data corresponds to a voltage sweep from 21.9V to 31.4V at a temperature T=21.50^{o}C and a diode driving current I_1= 25.820mA, the mode-hop-free range was graphically observed to be 2 FSR's, which, by calibration using the wavemeter, corresponds to 1.0GHz, which is a reasonably large range sufficient for our atomic cooling and trapping purposes.

Within this mode-hop-free range, the PZT voltage changes as follows:

Starting point of the mode-hop-free voltage range: 3rd curve from bottom → V_{start}=21.9+0.4*3=23.1V

End point of the mode-hop-free voltage range: 9th curve from top → V_{end}=31.4-0.4*9=27.8V

Thus this mode-hop-free range, in terms of PZT voltage, is from 23.1V to 27.8V, with a width of 27.8-23.1=4.7V. The slope of frequency with respect to PZT voltage is thus

$$df/dV = -\frac{1.0GHz}{4.7V} = -0.21\text{GHz/V} = -\frac{0.21GHz/V}{0.5GHz/FSR} = -0.42FSR/V$$

where the negative sign is due to the fact that the frequency decreases as voltage increases. Therefore, for this set of current and PZT voltage settings, the mode-hop-free tuning range is 4.7V, and the frequency is tuned linearly with voltage at a slope of 0.21GHz/V, which, in terms of the free spectral range of the Fabry-Perot cavity, is 0.42FSR/V.

The frequency vs. voltage plot shows that the frequency changes from 43709.6 GHz to 437310.6 GHz, this corresponds to a wavelength range from 686.011nm to 686.013nm, which does not include the desired wavelength 689.5nm. Therefore, this particular setting of the tuning parameters does not meet the experiment requirements.

Attempts were made to find any possible larger mode-hop-free ranges by sweeping the PZT over a larger range. A complete sweep of PZT voltage from 0V to 150V was carried out to find other mode-hop-free ranges besides the one from 23.1V to 27.8V. The only other significant mode-hop-free range found was when V is approximately 10~20V. The transmission curves over this voltage range was plotted in steps of 0.2V, as shown in figure x.

From the plot, the linearly relationship of frequency and voltage gets distorted even before each peak shifts for one FSR. Thus these mode-hop-free ranges are not as good as those from 23.1V to 27.8V. In conclusion, the 4.7V range from the calibration data was the best mode-hop-free tuning range possible for this current and temperature setting, T=21.50^{o}C and I_1=25.820mA. The fact that this mode-hop-free range fails to reach 689.5nm wavelength indicates that this current-temperature combination is not suitable for getting the desired laser frequency.

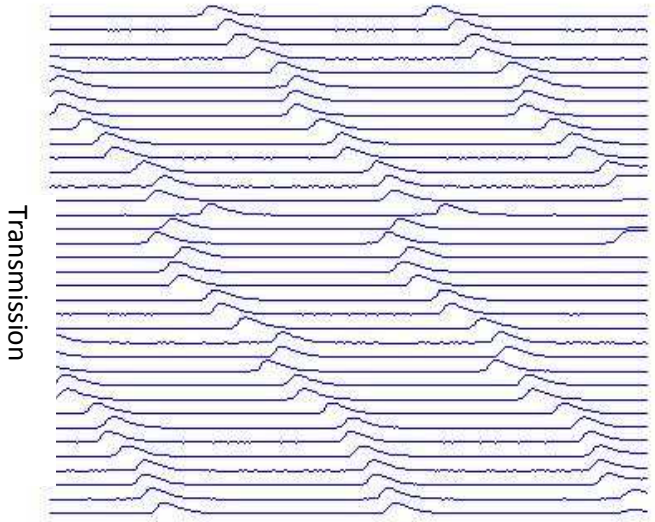

Figure x. The transmission curve for I_1=25.820mA, for PZT voltage ranging from 11.3V to 18.2V, in steps of 0.2V. As before, the x-axis of the plot is simply the time associated with the ramping of the PZT voltage. The

linearly relationship gets distorted even before each peak shifts for one FSR. Thus these mode-hop-free ranges are not as good as those from 23.1V to 27.8V.

Since I_1=25.820mA fails to reach the desired frequency, two other current values, I_2= 24.811mA and I_3=23.902 are implemented and a complete sweep of PZT voltage from 0V to 150V were carried out for each. Several mode-hop-free voltage ranges were found for each I, some ranges are very small, on the order of 0.5 V, and the others are relatively larger. Figure 15 and 16 show, for I_2 and I_3 respectively, a histogram with different mode-hop-free ranges found over the 0~150V voltage sweep, along with the transmission curves and the frequency vs. voltage plot for the largest mode-hop-free range seen from the histogram.

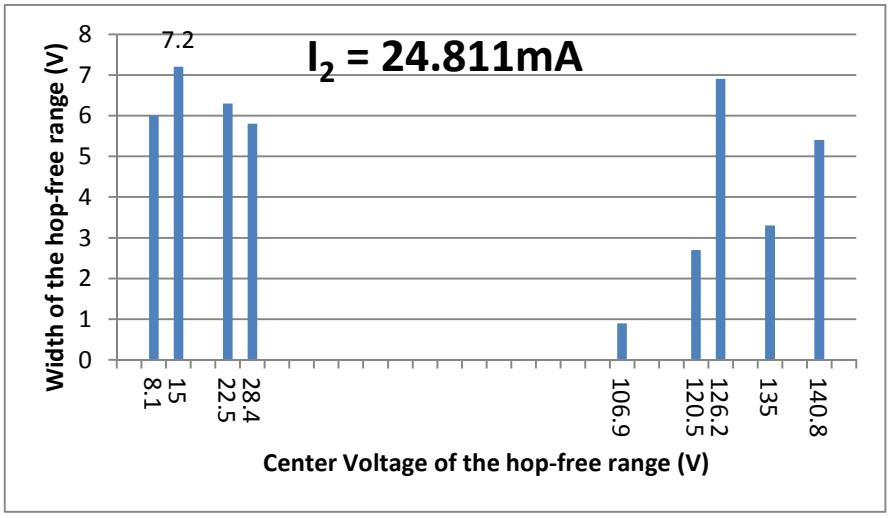

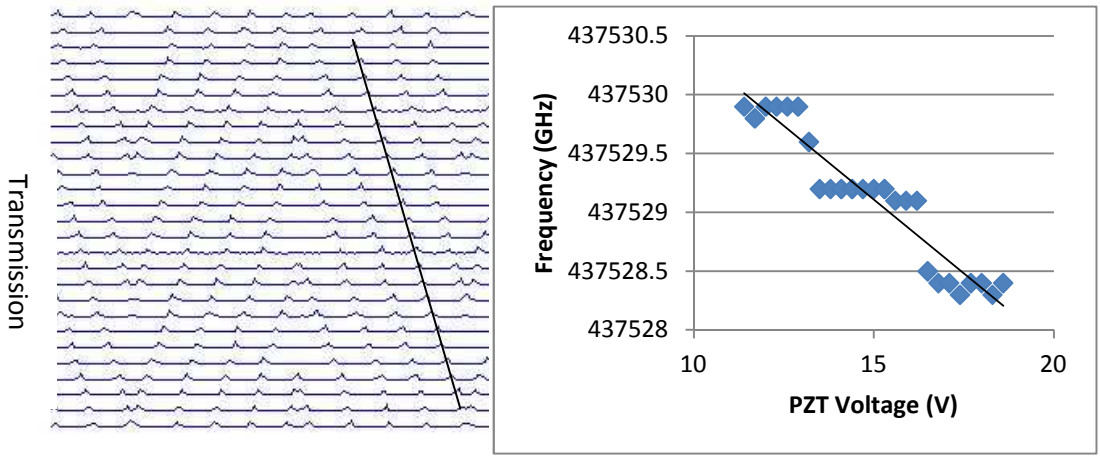

Figure 15. Observation of the mode-hop-free PZT tuning ranges for fixed currents I_2=24.811mA and fixed temperature T=21.50°C.

(a) shows the distribution of hop-free PZT voltage ranges over the entire 0~150V sweep. There are several major hop-free ranges larger than 5V, with the largest one centered at 15V, with a hop-free tuning range of 7.2V (b) shows the transmission curves for this range, with a voltage step of 0.3V. (c) shows the frequency read from the wavemeter, but to a low precision. This frequency range corresponds to wavelengths around 685.67nm. It can then be observed that the frequency change for this hop-free range is 1.6GHz, which corresponding to about 3 FSR. A linear fit is done to the freq vs. V plot and the slope is df/dV=-0.25GHz/V.

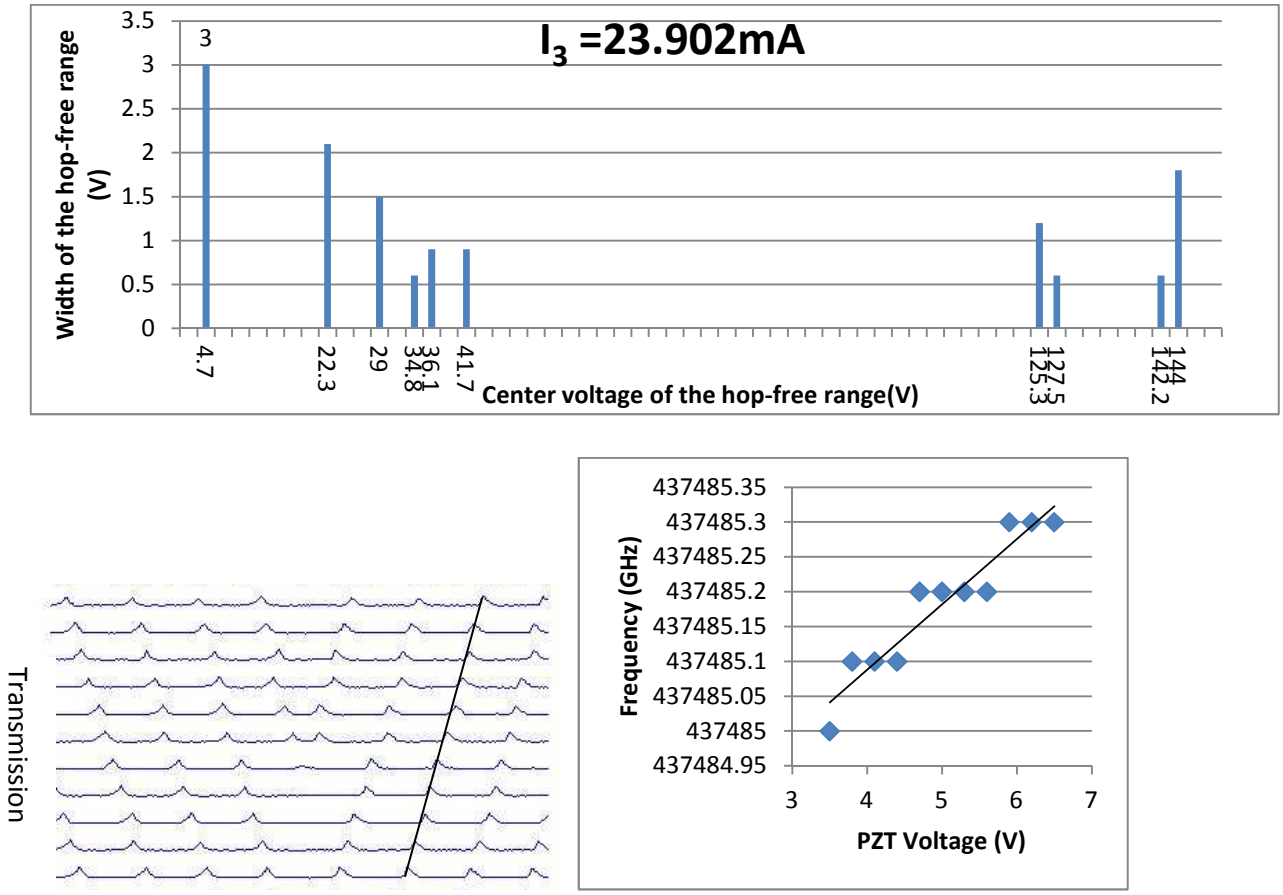

Figure 16. Observation of the mode-hop-free PZT tuning ranges for fixed current I_3=23.902mA and temperature T=21.50°C.

(a) shows the distribution of hop-free PZT voltage ranges over the entire 0~150V sweep. There are three major hop-free ranges larger than 1.5V, centered at 4.7V, 22.3V and 144V respectively. The one at 4.7V has the largest tuning range, about 3.0V. (b) shows the transmission curves for this range, with a

voltage step of 0.3V. (c) shows the frequency read from the wavemeter, but to a low precision. This frequency range corresponds to a wavelength 685.74nm. It can then be observed that the frequency change for this hop-free range is 0.3GHz, which corresponding to 0.6 FSR. A linear fit is done to the freq vs. V plot and the slope is df/dV=-0.09GHz/V.

From the figures, it is clear that I_3 =23.902mA have significantly narrower mode-hop-free PZT tuning range than I_1, which was only 1 FSR. It also has a much lower magnitude of df/dV slope, -0.09GHz/V, which makes PZT tuning rather inefficient. However, I_2=24.811mA behaves much better. It has a mode-hop-free tuning range of over 1.6 GHz, which is more than 3 FSR. This is so far the largest PZT tuning range we have got for any current settings.

The df/dV slope is -0.25GHz/V, which enables efficient frequency tuning within small PZT voltage ranges. Unfortunately, both I_2 and I_3 results in wavelengths around 685.7nm, and thus both fail to reach the required value. Other attempts have been made to increase the wavelength by changing the ECDL parameter settings, but the wavelength is always around 686nm, and is unable to reach the desired 689.5nm.

6. Current characterization

As introduced in Chapter 1, due to the semiconductor lattice structure of the gain medium of diodes, the output frequency of a diode laser decreases when the driving current increases, which correspond to a decrease in wavelength. The dependence of frequency on current above the ECDL threshold current (19.0mA) is plotted in Figure 17.

As shown in the figure, the frequency decreases as current increases, as expected. The rate of change is seen to be -6.434GHz/mA.

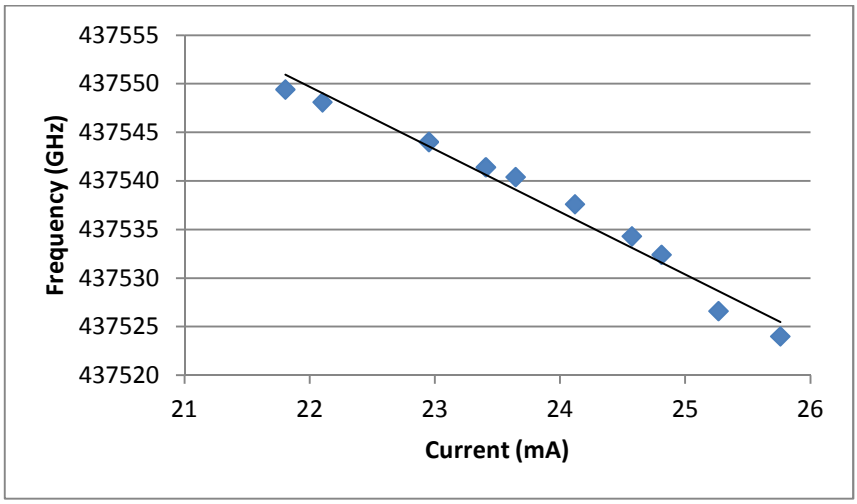

Figure 17. Above the threshold current, frequency changes linearly with current. A linear fit to the plot indicate a slope of -6.434 GHz/mA.

Note that in Chapter 5, 3 current values I_1=25.820mA, I_2=24.811mA and I_3=23.902mA were used for the PZT voltage sweeps. The wavemeter reading for these three current setting indicates that the frequencies of these settings were around f_1=437310GHz, f_2=437520GHz, f_3=437483GHz respectively. The 2nd and 3rd set of data implies that the frequency has increased as the current increase from I_3 to I_2, which is against the general trend that df/dI <0. Since the two frequency values are rather close, and only one set of data is taken for each, the deviation from theoretical prediction may be due to random experimental errors.

7. Conclusion

In conclusion, we have constructed and characterized an Extended Cavity Diode Laser that may have immediate applications in the laser cooling and trapping system for Strontium atomic samples. The power of this laser can reach up to 5 mW. This laser is highly single-frequency, is tunable around a wavelength of 686nm, and has mode-hop-free tuning ranges as long as 1.6GHz.

One limitation of the laser is that its tuning range is relatively narrow compared to some other lasers being built for similar purposes. For instance, a 689nm Short Extended Cavity Diode Laser built in our lab in 2008 had a mode-hop-free tuning range of at least 20 GHz [1]. However, the free tuning range of our ECDL should still be sufficient for its purposes. Another limitation of the laser is that it fails to reach the desired 689.5nm wavelength.

The performance of this ECDL may be enhanced with the following improvements. Firstly, it is possible to explore tuning the laser with PZT and current simultaneously to achieve an even larger tuning range. This concept has been explored before [13] and has been shown to be effective in extending the mode-hop-free tuning ranges of ECDLs.

Secondly, a transparent cover, such as a Plexiglass box, could be made to shield the ECDL. Although several attempts has been made to put the ECDL in a thermally and mechanically stable environment, such as by adding a temperature control unit and an aluminum base anchored to the vibration-proof table, the temperature drift of the air immediately around the optical mounts make still disturb the ECDL operation. Furthermore, the dusts and other impurities in the air may cause damage to the optics. Therefore, with a cover that shields the system from the air but allows the output light to go through, the laser performance may be enhanced.

Bibliography

[1] A. Dunn, *A Novel Extended-Cavity Diode Laser in Red Wavelengths*. Undergraduate thesis, 2008.

[2] S. B. Nagel, *A Narrow Linewidth Diode Laser System for Strontium Laser Cooling Applications*. Master thesis, 2004

[3] F.B. Dunning and R.G. Hulet. Atomic, *Molecular, and Optical Physics: Electromagnetic Radiation*. Academic Press, 1997.

[4] W. B Phillips, *Laser Cooling and Trapping of Neutral Atoms*, *Laser Manipulations of Atoms and Ions*, edited by E. Arimondo, W. D. Phillips, and F. Strumia, Proceedings of the International School of Physics, "Enrico Fermi", p. 289.

[5] W. D. Phillips and H. J. Metcalf, Physical Review Letters, 49, 1149. 1982

[6] S.B. Nagel, C.E. Simien, S. Laha, P. Gupta, V.S. Ashoka, and T.C. Killian. Magnetic *trapping of metastable $^3P_2$ atomic strontium*. Physical Review A, 67, 011401(R), 2003.

[7] Y. N. Martinez de Escobar, *Bose-Einstein Condensation of 84-Sr*. Doctoral thesis, 2010.

[8] E. Hecht and A. Zajac. *Optics*. Addison-Wesley Publishing Company, Reading, Massachusetts. Adelphi University, 1979.

[9] C. Palmer, *Diffraction Grating Handbook*. Newport Corporation. New York, 2005.

[10] M. G. Littman and H. J. Metcalf, *Spectrally Narrow Pulsed Dye Laser Without Beam Expander*. Applied Optics, Vol. 17, p2224, 1978.

[11] C. J. Erickson, M. Van Zijll, G. Doermann, and D. S. Durfee, *An Ultrahigh Stability, Low-noise Laser Current Driver with Digital Control*. Review of Scientific Instruments, 79, 2008.

[12] H. Kogelnik, T. Li, *Laser Beams and Resonators*. Proceedings of the IEEE, VOL. 54, NO. 10, 1966.

[13] J. Hult, I.S. Burns, C.F. Kaminski. *Wide-bandwidth mode-hop-free tuning of extended-cavity GaN diode lasers*. Applied Optics (44), 2005.

Appendix 1. Mechanical Drawings of Self-fabricated Components of the ECDL

Diode Holder

Brass
Qty: 1, second view
All units in inches
tolerance +/- 0.010" unless otherwise specified

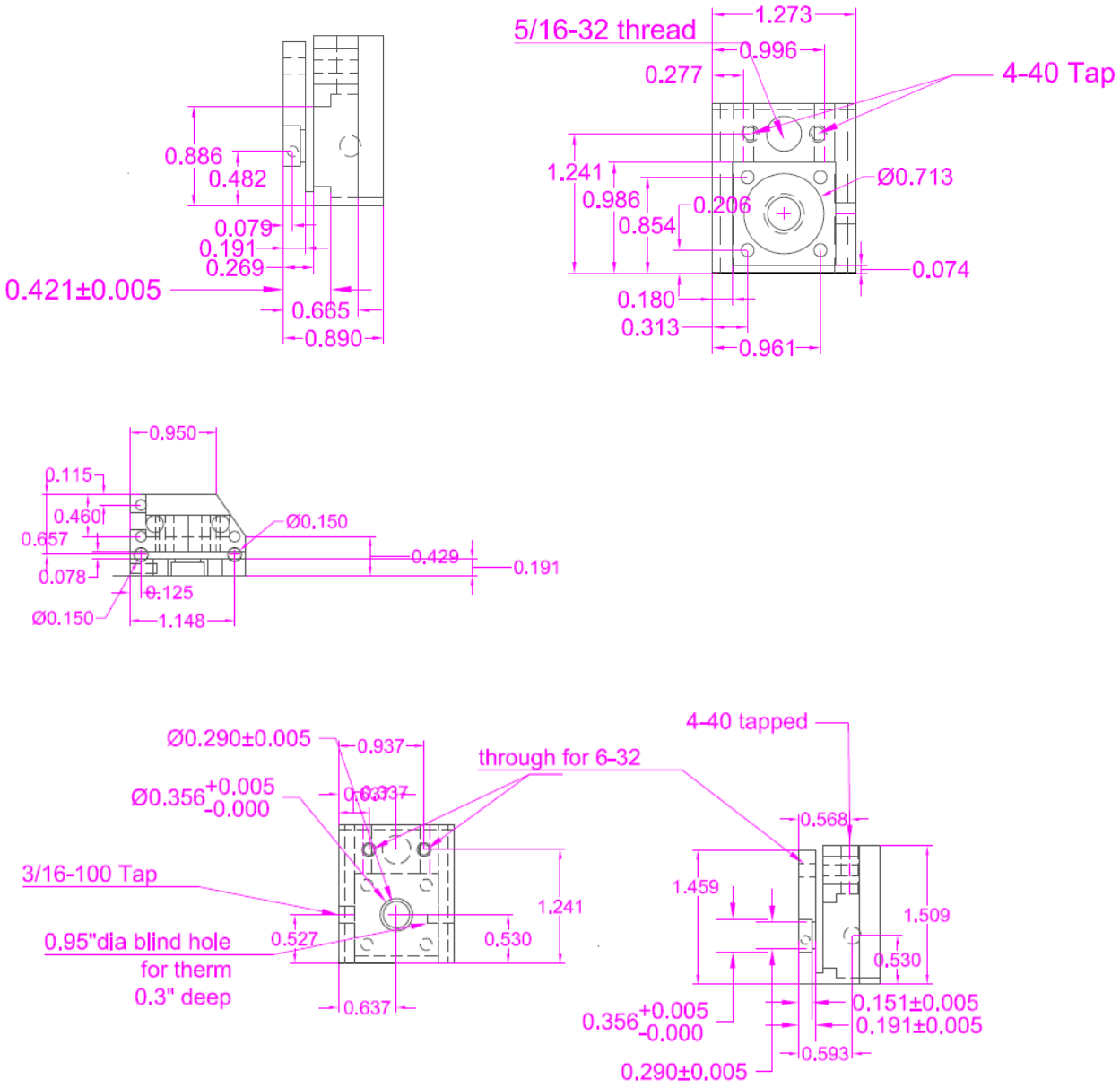

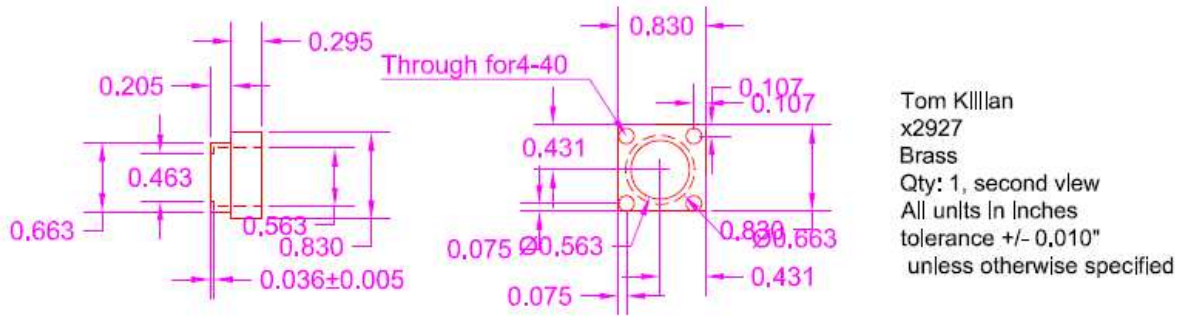

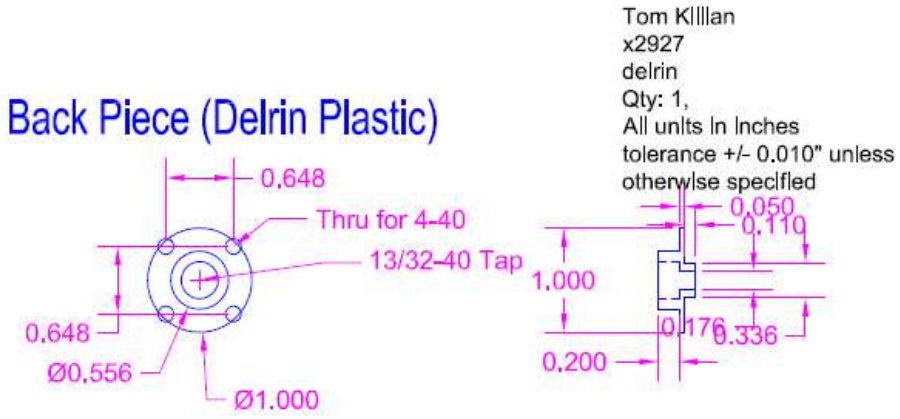

Diode Holder Back Piece and Le

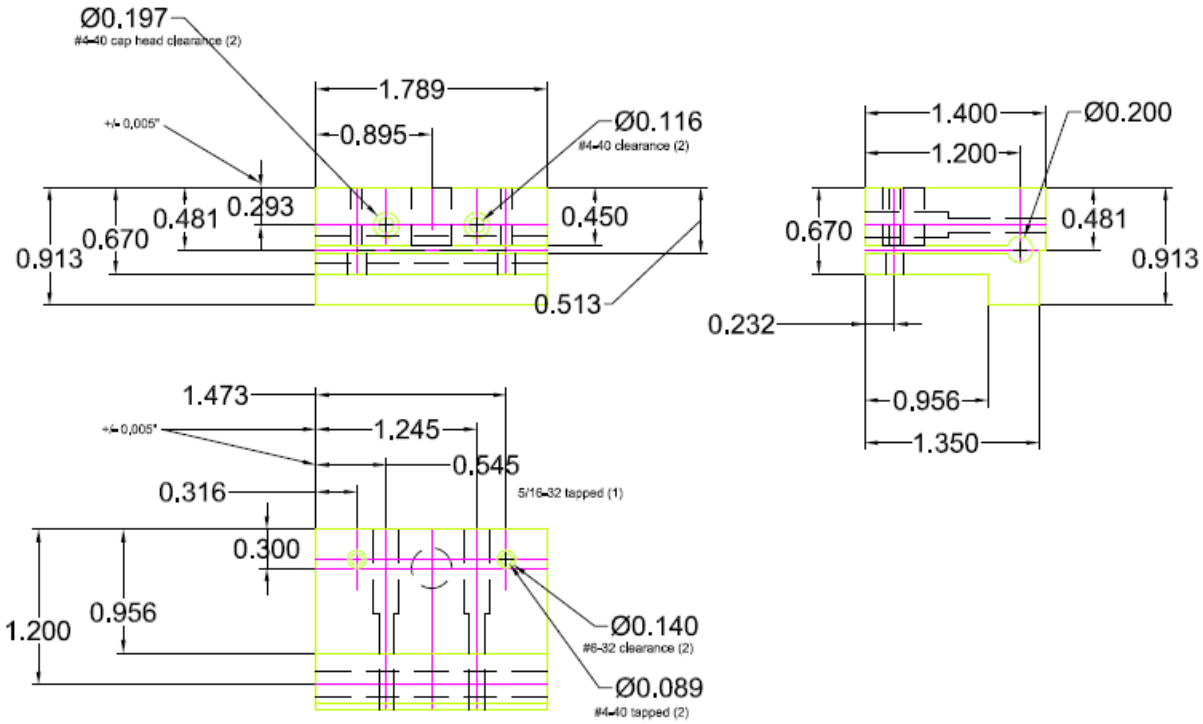

Grating Holder

Mirror Mount

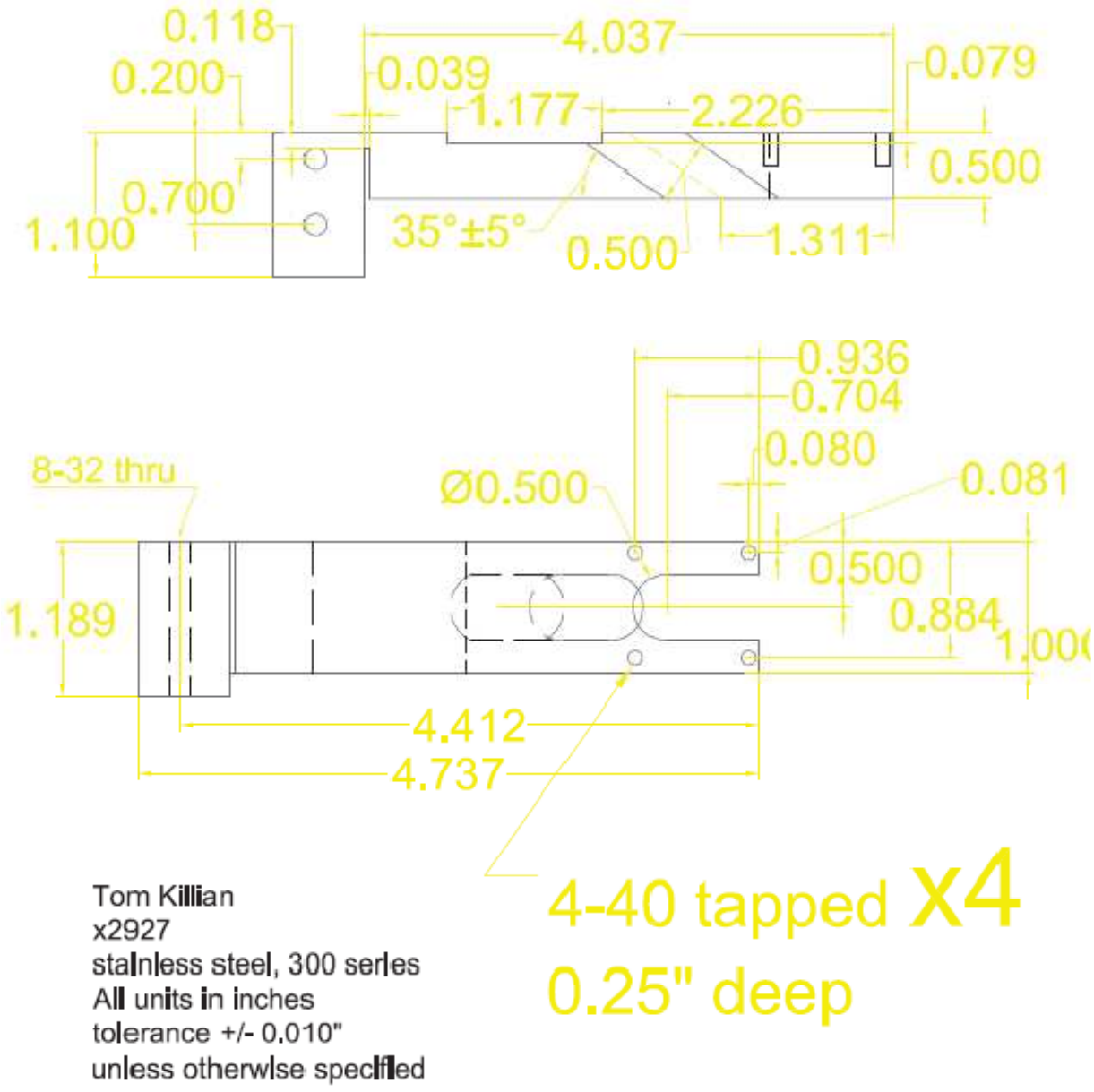

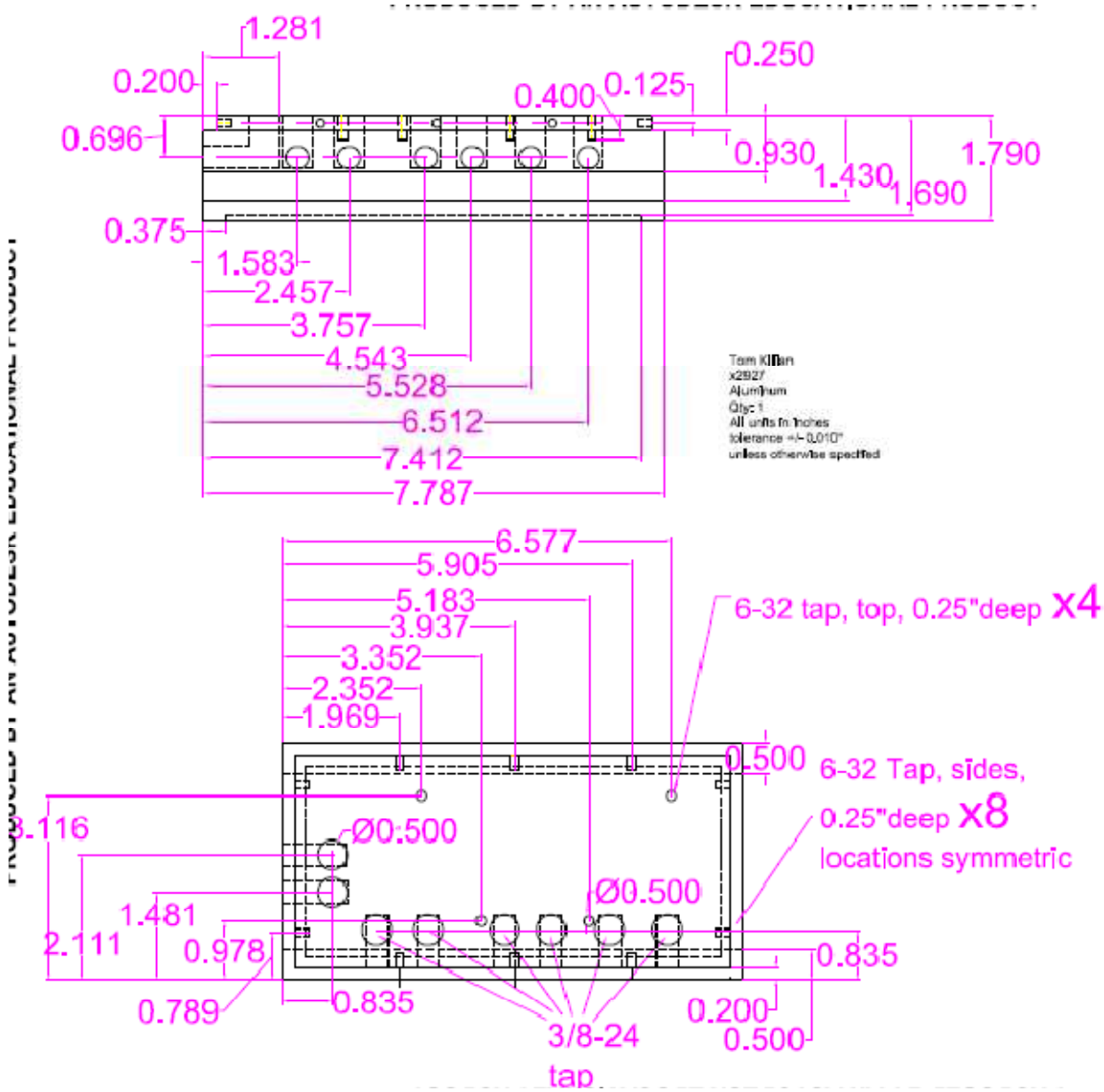

Aluminum Base

Appendix 2. List of Components for the Current Driver Circuit

Newark Part Number	Subcircuit	Device	Specific Type	Quantity	Value		Aditional Specs
LM399HLT-ND	Dig Set Pnt	Diode	LM399	**1**			Zener, 6.95 V drop
89M6889	Dig Set Pnt	Resistor	TNPW04027501DT9	**1**	7.5 kΩ		precision, low temp coef
T101MH9AVBE	Volt Reg	Switch	T101MH9AVBE	**1**			
96K4787	VR/MI	Capacitor		**2**	1 µF		ceramic
84K8407	PF/VR/MI/CR/CM	Capacitor	1206	**11**	10 µF		surface-mount ceramic
70K9164	PF/MI/CR/CM	Capacitor	1206	**7**	.01 µF		surface-mount ceramic
69K9627	CR/PF	Inductor	S1210	**3**	100 µH		Ferrite core shielded, surface-mount
01F9174	Set Pnt	Trim-Pot		**1**	5 kΩ		
69K9627	CR/VR	Inductor	S1210	**1**	100 µH		
19P8315	Current Reg	Op-Amp	AD8671	**1**			
38C7430	Volt Reg	Transistor	MMBT2907A	**1**			
59M6997	Mod Inp	Resistor		**1**	47 Ω		impeadence matching
32R8927	Volt Reg	Capacitor		**2**	220 µF		low leakage,radial,aluminum,
94M5671	SP/VR	Capacitor	1206	**3**	22 µF		ceramic, surface mount
41K4771	Volt Reg	Regulator	LM340-12	**1**	+12V		Suface mount LDO/Linear
75M9218	Power Filter	Capcitor		**2**	47 µF		suface-mount, tantulum
41K6357	Volt Reg	Regulator	LM7912	**1**	-12 V		Suface mount LDO/Linear
39K0872	CR/CM	Resistor	1206	**5**	10 kΩ		1/8 W thick-film chip, surface-mount
84M8463	VR/MI	Resistor	TNPW0805	**9**	1 kΩ		Vishay, precision, accuracy
89M6867	Set Pnt	Resistor	1206	**2**	3 kΩ		1/8 W thick-film chip
05R5979	Volt Reg	Diodes		**3**			Protection for LM317
15R1531	Volt Reg	Resistor	1206	**1**	1.5 Ω		1/8 W thick-film chip
58K9477	Current Reg	MOSFET	NDS0605	**1**			
19M0999	MI/CM	Op-Amp	AD8672	**2**			
98K0094	Current Reg	Resistor	Y1169100R000T9R	**2**	100 ohm		
59M6948	Current Reg	Resistor		**1**	100 ohm		
51R8341	Volt Reg	Resistor	TNPW0805	**1**	2.74 kΩ		Vishay, precision, accuracy
64R5476	Volt Reg	Resistor	1206	**1**	5.6 kΩ		thick-film chip, surface-mount
35R3030	Power Filter	Connector	SDF-50J	**1**			5-pin
41K4771	Power Filter	Regulator	LM340-12	**1**			fixed +12 V Suface mount available
41K6357	Power Filter	Regulator	LM7912	**1**			fixed-12 V Suface mount available
	PF/SP	Jumper		**2**			
45J0740	Volt Reg	Volt Reg	LM317	**1**			adjustable
70K9166	Volt Reg	Capacitor		**1**	.1 µF		ceramic
T101MH9AVBE	Volt Reg	Switch	T101MH9AVBE	**1**			
59M6997	Mod Inp	Resistor		**1**	47 Ω		impeadence matching
42K8695	MI/CR/CM	Connector	5227161-1	**3**			BNC RF
96M1368	Current Reg	Capacitor	08051C822KAT2A	**1**	8.2 pF		